Dynamic Simulation of Three-Phase Separator for Oil and Gas Processing Operation using Aspen HYSYS

ABSTRACT

The transient dynamics of three-phase separators play a critical role in upstream oil and gas production facilities. However, conventional steady-state design methodologies rarely account for time-dependent operational effects with sufficient rigor.. In this study, a dynamic simulation framework for a horizontal three-phase separator was developed and evaluated using Aspen HYSYS Dynamics to investigate time-dependent separation behaviour under realistic operating disturbances. The model integrates mass, momentum, and energy balances with thermodynamically consistent phase equilibrium calculations and embedded process control logic. The separator performance was analysed using field operating data comprising a total inlet molar flow rate of 21.15 kmol·h^{-1}, separator pressure of 350 kPa, feed temperature of 337.65 K, gas mole fraction of 0.41, oil mole fraction of 0.44, water mole. The deviation between the field data and the simulated results were gas outlet rate (1.4 %), oil out rate (1.6 %), water outlet rate (1.5 %), separator pressure (0.2 %), and total liquid level (1.4 %). The low deviations confirms that the dynamic model reliably reproduces vapor–liquid–liquid phase separation behaviour, gravitational separation efficiency, controller interaction with separator inventories, and steady operational throughput under realistic field conditions. The results further indicate that separator efficiency and operational stability are governed by coupled thermodynamic and hydraulic interactions that can only be fully resolved through dynamic modelling. The developed framework therefore provides a robust basis for operational optimization, control strategy development, and design support for upstream oil and gas production facilities.

Keywords: Three-phase separator; Dynamic simulation; Aspen HYSYS; Multiphase separation; Oil and gas processing

1.0 Introduction

Three-phase separators are safety-critical process units in upstream oil and gas production, responsible for the initial separation of produced fluids into gas, oil, and water phases prior to downstream handling and export (Figures 1 and 2). Their operational performance directly affects product quality, operational safety, equipment integrity, environmental compliance, and overall production economics (Arnold & Stewart, 2008; Sinnott & Towler, 2019;Mokhatab et al., 2019). In field operation, separators are continuously exposed to transient disturbances arising from well routing changes, choke adjustments, reservoir decline, slugging, and control actions. These disturbances induce time-dependent variations in flow rate, pressure, temperature, and phase composition, which cannot be adequately represented using steady-state design assumptions (Hasan & Kabir, 2010; Sinnott & Towler, 2019).

.

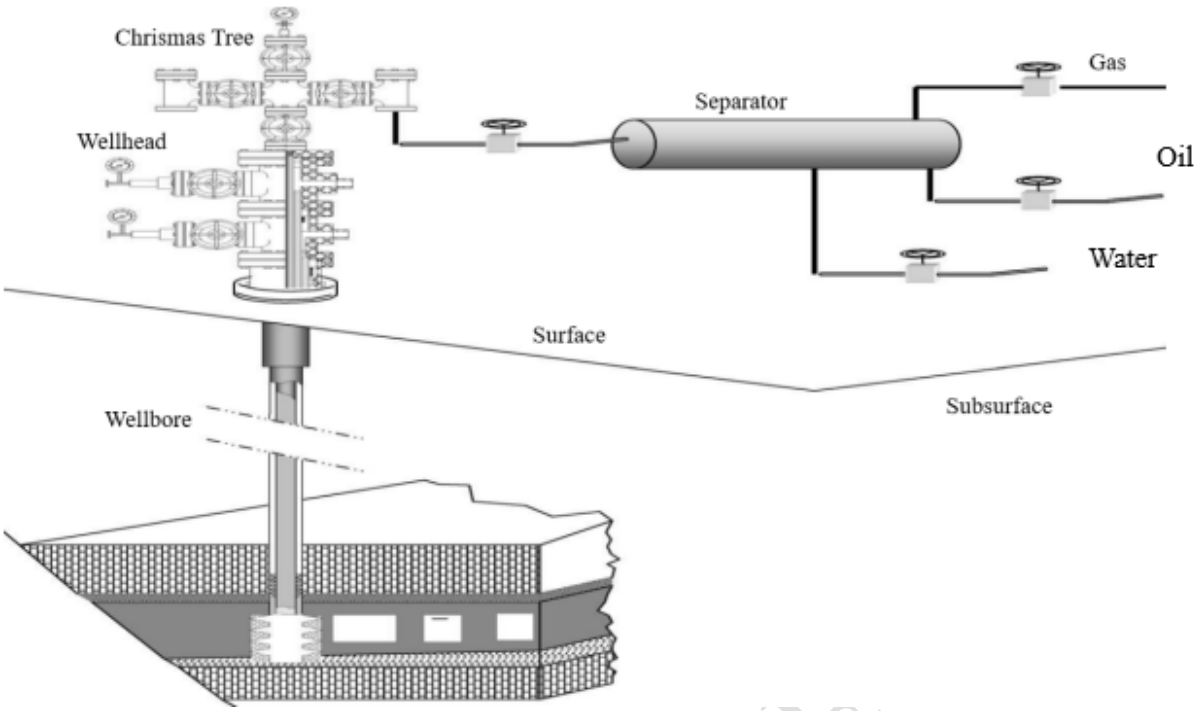

Figure 1. Petroleum production system

Historically, the design and performance evaluation of three-phase separators have relied on steady-state correlations and residence-time criteria developed under idealized flow conditions (Arnold & Stewart, 2008; Sinnott & Towler, 2019). Although these methodologies remain appropriate for preliminary sizing and conceptual design, they are inherently limited in their ability to represent dynamic phenomena such as liquid–liquid interface oscillations, control-loop interactions, transient phase carryover, and delayed phase disengagement. As a result, steady-state models provide limited guidance for operational optimization and risk mitigation under realistic field operating conditions. To overcome these limitations, previous investigations have increasingly employed dynamic modelling techniques to three-phase separators. Computational fluid dynamics (CFD)-based studies have delivered detailed characterization of internal hydrodynamics and phase distribution within separator vessels (Gomez et al., 2010; Frank et al., 2015). However, the substantial computational demand associated with CFD limits its practical application primarily to design-stage analysis and constrains its routine use for transient operational studies or control-oriented performance evaluation.

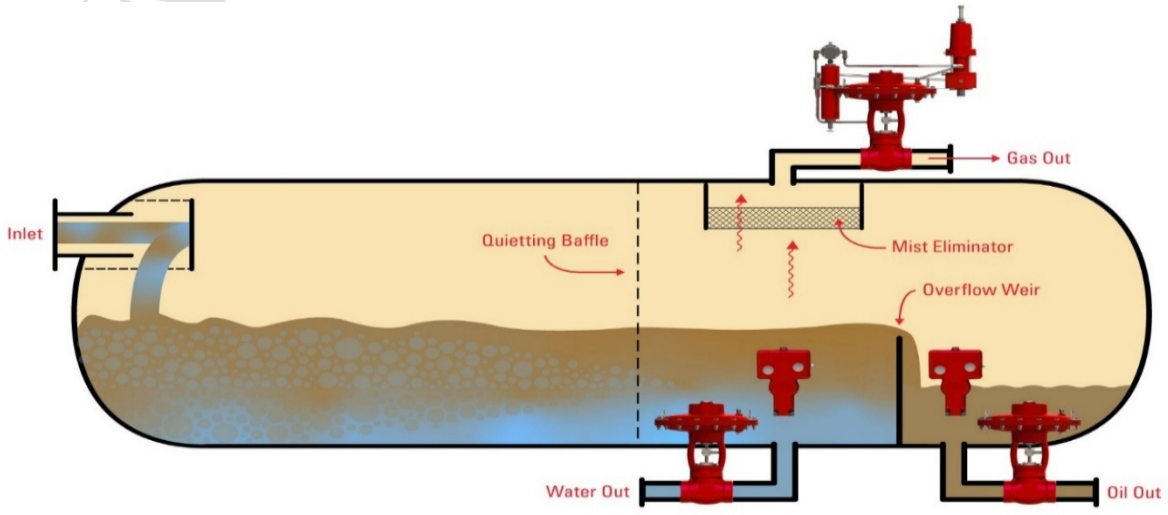

Figure 2 Horizontal Three-Phase Separator

Process-level dynamic simulation using commercial process simulators has emerged as a practical alternative to high-fidelity CFD, enabling the integration of thermodynamics, phase equilibrium, hydraulic behaviour, and embedded control logic within a unified modelling environment (Luyben, 2013; Sinnott & Towler, 2019). Such platforms provide a computationally efficient framework for evaluating transient process responses while maintaining thermodynamic consistency. Despite these advancements, three recurring limitations are evident in the existing body of dynamic separator studies including many models are developed for highly specific field cases, limiting their generalizability and transferability to other operating envelopes. Fluid characterization is frequently simplified, particularly with respect to heavy-end hydrocarbons, even though pseudo-component thermophysical properties strongly influence phase behaviour, liquid holdup, and separation efficiency (Whitson & Brulé, 2000; Pedersen & Christensen, 2007). Transient analyses are often restricted to isolated disturbances or single-variable changes, without systematically quantifying the coupled effects of flow rate, pressure, and temperature under control-stable operating conditions (Luyben, 2013). Consequently, a gap persists between dynamic separator modelling as demonstrated in the literature and and the development of a generalized, operationally robust framework capable of supporting sensitivity analysis, optimization, and future digitalization initiatives. The present study addresses these gaps through the development of a control-stable dynamic simulation framework for a horizontal three-phase separator using Aspen HYSYS Dynamics. In contrast to prior case-specific implementations, the model employs a generalized pseudo-component representation of heavy hydrocarbon fractions, enabling thermodynamically consistent prediction of phase behaviour across an extended range of operating conditions (Whitson & Brulé, 2000). Explicit pressure and liquid-level control strategies are embedded to ensure realistic transient responses and to isolate intrinsic process dynamics from control-induced artefacts (Luyben, 2013). A systematic dynamic sensitivity analysis is performed with respect to inlet molar flow rate, operating pressure, and temperature. Rather than evaluating these variables independently under steady-state assumptions, their transient impact on separation efficiency, phase recovery, and system stability is quantified under realistic dynamic operation. This approach facilitates the identification of nonlinear process responses, diminishing returns associated with pressure escalation, and temperature-driven shifts in liquid recovery that are not observable using steady-state models (Sinnott & Towler, 2019). The key novelty of this work lies in advancing beyond demonstration-level dynamic simulation toward a generalized, sensitivity-driven framework that integrates rigorous heavy-end pseudo-component modelling with control-consistent transient analysis. Unlike previous studies that focused on isolated scenarios or simplified fluid systems, this approach provides operationally actionable insight into separator performance envelopes and establishes a scalable foundation for future optimization, digital monitoring, and advanced control applications in upstream oil and gas processing.

2.0 Methodology

2.1 Dynamic Simulation Framework with Control Stabilization

A control-stabilized dynamic simulation framework was developed to investigate the transient behaviour of a horizontal three-phase separator under realistic upstream production conditions. The model was implemented in Aspen HYSYS Dynamics, which solves time-dependent mass, momentum, and energy conservation equations coupled with rigorous vapor–liquid–liquid equilibrium (VLLE) calculations (Aspen Tech, 2022; Sinnott & Towler, 2019). The modelling workflow integrated steady-state initialization, dynamic conversion, embedded process control, disturbance testing, and structured data acquisition to ensure numerical stability and reproducibility. Simulations were executed on a high-performance computational workstation

capable of efficiently resolving stiff differential–algebraic equation systems typical of dynamic process simulations (Biegler, 2010; Luyben, 2013). Automated data logging recorded time-dependent variations in pressure, temperature, phase flow rates, liquid holdup, and controller responses. Simulation outputs were exported for post-processing and statistical analysis using external scientific computing tools.

2.1.1 Steady-State Model Development

A steady-state process flowsheet representing a field-scale horizontal three-phase separator was first constructed in Aspen HYSYS. The Peng–Robinson equation of state (PR-EOS) was selected as the thermodynamic property package due to its proven applicability for hydrocarbon production systems (Pedersen & Christensen, 2007). The feed stream composition included light hydrocarbon together with lumped heavy fractions components represented by pseudo-components (C12+, KA1, KA2, and KA3). Nominal operating conditions were defined at a separator pressure of 350 kPa, temperature of 337.65 K, and an initial liquid holdup of approximately 50 %. The separator vessel geometry, internal configuration, and outlet streams for gas, oil, and produced water were specified according to standard horizontal three-phase separator design practice (Arnold & Stewart, 2008).

2.1.2 Conversion to Dynamic Mode

The converged steady-state model was converted to dynamic mode using the Aspen HYSYS Dynamics. Vessel volumes, hydraulic capacities, and liquid level boundaries were defined to enable time-dependent accumulation within the separator. Dynamics pressure flow relationships were specified for all inlet and outlet valves to reproduce realistic hydraulic resistance and flow behaviour (Luyben, 2013).

2.1.3 Implementation of Control Architecture

To replicate field operating practice, pressure and liquid levels were regulated using embedded proportional–integral–derivative (PID) controllers. The separator gas outlet valve was installed to regulate the vessel pressure at its nominal setpoint of 350 kPa. Independent level controllers were implemented to maintained total liquid level and oil–water interface position through modulation of oil and water outlet valves. The PID controller parameters (proportional gain, integral time, and derivative action) were tuned using standard process control tuning guidelines to achieve stable operation without excessive oscillation (Seborg et al., 2017).

2.1.4 Baseline Dynamic Initialization

The dynamic simulation was initialized from the converged steady-state solution. The system operated under closed-loop control until pressure, interface levels, and outlet flow rates stabilized within predefined tolerances. This procedure eliminated artificial numerical transients prior to disturbance testing.

2.1.5 Transient Disturbance Testing

Controlled disturbances were introduced individually to evaluate intrinsic separator dynamics while maintaining active control loops. The investigated variables included inlet molar flow rate, feed temperature, and pressure. Each disturbance was applied independently to isolate process response from control instability.

2.1.6 Data Acquisition and Analysis

Dynamic variables such as gas, oil, and water production rates, separator pressure, liquid holdup and interface levels, phase compositions, and control valve positions were recorded continuously using automated logging functions during simulation. The resulting time-series datasets were exported for post-processing and sensitivity analysis using external scientific

computing tools. This procedure enabled quantitative evaluation of separator stability, phase recovery efficiency, and transient response characteristics under varying operating conditions. The modelling framework allows systematic evaluation of separator responses to operational disturbances such as production fluctuations, well switching, and variable reservoir conditions. This approach provides a practical platform for analysing transient separator performance and assessing operational stability systems.

2.2 Generalized Thermodynamic Representation Using Structured Hypothetical Components

Complex crude oil composition was represented using structured hypothetical pseudo-components within the Aspen HYSYS fluid characterization framework. Heavy hydrocarbon fractions were modelled using lumped components defined by thermophysical properties such as molecular weight (MW), normal boiling point (NBP), critical temperature (Tc), critical pressure (Pc), liquid density, and acentric factor (ω). When experimental measurements were unavailable, critical properties and acentric factors were estimated using petroleum characterization correlations embedded within the simulator. This approach enabled consisted thermodynamic modelling without reliance on field-specific compositional assays.

2.2.1 Heavy-End Fluid Characterization

The feed stream composition was defined in the process simulation environment by specifying the light hydrocarbons & permanent gas components (C_1–C_{10}) along with structured hypothetical components representing the heavy-end fraction (e.g., C12+, KA1, KA2, & KA3). Each pseudo-component was created in Aspen HYSYS using the Hypothetical Component Manager, where thermodynamic properties were calculated from correlations based on molecular weight (MW), normal boiling point (NBP) & liquid density at reference conditions. Critical properties for the hypothetical components were generated using empirical petroleum correlations embedded in the software. Equations 1 and 2 present the correlations for critical temperature (T_c) and critical pressure (P_c) of the pseudo-components, based on molecular weight and boiling point relationships.

Critical temperature correlation

$$T_c = f(T_b, MW) \quad (1)$$

Critical pressure correlation

$$P_c = g(T_b, MW) \quad (2)$$

where: T_b= normal boiling point and MW= molecular weight

The acentric factor (ω), presented in Equation 3, characterizes the deviation of a molecule from spherical symmetry and significantly influences phase behaviour. In this study, it was determined using established vapor-pressure correlations.

Acentric factor correlation

$$\omega = -\log_{10}(P_r^{sat}) - 1 \quad (3)$$

where: P_r^{sat} is the reduced vapor pressure evaluated at a reduced temperature $T_r = 0.7$ as presented in Equation 4.

$$P_r^{sat} = \frac{P^{sat}}{P_c} \quad (4)$$

These property correlations enable consistent thermodynamic representation of heavy fractions without requiring detailed compositional laboratory analysis.

2.2.2 Phase Equilibrium Modelling

Vapor–liquid equilibrium (VLE), liquid–liquid equilibrium (LLE), and density calculations were performed using the Peng–Robinson equation of state (PR-EOS) in the Simulation Basis

Manager, which is commonly applied for hydrocarbon mixtures due to its reliability in predicting phase behaviour of hydrocarbon mixtures encountered in petroleum production and processing operations across a wide range of pressures and temperatures.
The Peng–Robinson equation of state used in the simulation is expressed as Equation (5)

$$P = \frac{RT}{V-b} - \frac{a(T)}{V(V+b)+b(V-b)} \quad (5)$$

where: P= pressure; T= temperature; V= molar volume and R= universal gas constant; $a(T)$= temperature-dependent attractive parameter; b= co-volume parameter
The temperature dependent attractive parameter is given in Equation 2.6

$$a(T) = a_c\alpha(T) \quad (6)$$

The attraction parameter at the critical point, which represents the magnitude of intermolecular attractive forces when the fluid is at its critical state, is given in Equation (7).

$$a_c = 0.45724\frac{R^2T_c^2}{P_c} \quad (7)$$

The co-volume parameter is given in Equation 8

$$b = 0.07780\frac{RT_c}{P_c} \quad (8)$$

The temperature-dependent factor $\alpha(T)$ is a dimensionless, temperature-dependent function that modifies the attraction parameter at temperatures other than the critical temperature, thereby accounting for the influence of temperature on intermolecular attractive forces, as shown in Equation 9.

$$\alpha(T) = \left[1 + \kappa\left(1-\sqrt{\frac{T}{T_c}}\right)\right]^2 \quad (9)$$

where;

$$\kappa = 0.37464 + 1.54226\omega - 0.26992\omega^2$$

The PR-EOS formulation enables the simulator to determine phase distribution, vapor fraction, and equilibrium compositions required for separation modelling.

2.2.3 Transport Property Evaluation

Transport properties required for multiphase process simulations including liquid density, dynamic viscosity, heat capacity (Cp) and thermal conductivity, were calculated automatically within the Aspen HYSYS thermodynamic framework using corresponding states states methods and embedded empirical correlations. For hydrocarbon mixtures, the fluid density can be obtained from the selected equation of state through the compressibility factor (Z), as expressed in Equation 10.

$$Z = \frac{PV}{RT} \quad (10)$$

from which molar density can be obtained as

$$\rho = \frac{P}{ZRT} \quad (11)$$

Mixture heat capacity and viscosity were calculated using component contribution methods and mixing rules implemented within the property package. These property predictions allow accurate estimation of gas evolution, phase densities, interfacial stability, liquid holdup and residence time within the separator during dynamic operation. The prediction of mixture viscosity follows generalized corresponding-states relationships of the form as expressed in Equation 12

$$\mu = f(T,P,MW) \quad (12)$$

where; viscosity depends on temperature, pressure, and molecular weight distribution of the fluid mixture.

By structuring the heavy hydrocarbon fraction into representative pseudo-components, the simulation preserves the essential compositional characteristics of the fluid while maintaining numerical stability and computational efficiency.

2.3 Separator Configuration and Internal Representation

A three-phase separator was modelled in Aspen HYSYS Dynamics to represent a horizontal cylindrical production separator typical of petroleum processing operations. The unit was added into the process flowsheet and configured for simultaneous separation of gas, oil, and aqueous phases. Vessel geometry, including internal diameter, overall length, and horizontal orientation, was defined within the equipment configuration environment to enable accurate calculation of phase holdup, liquid levels, and gas–liquid interface positions during dynamic simulation. Separator internals were represented through the following modelling assumptions:

1. **Momentum-Dissipating Inlet Diverter:**

   The feed stream entered the separator through the inlet nozzle with an upstream pressure-control valve regulating inlet pressure. This setup reduced the momentum and kinetic energy of the incoming fluid, simulating the function of a physical inlet diverter by minimizing jet impact and promoting efficient separation of gas, oil, and water phases.

2. **Gravity Settling Zones:**
   Phase separation was governed primarily by gravitational settling within the vessel. Phase distribution among gas, hydrocarbon liquid, and aqueous liquid streams was determined using equilibrium flash calculations coupled with vessel holdup correlations.

3. **Oil–Water Interface Weir:**
   A liquid level controller (LIC) located at the heavy-liquid outlet regulated the oil–water interface height. The controller adjusted the water outlet valve to maintain the specified interface level and prevent phase carryover.

4. **Gas-Phase Mist Extractor:**

Mist elimination was represented by assuming negligible liquid entrainment in the gas outlet. Equilibrium phase separation ensured that the gas phase exited through the overhead stream with minimal liquid carryover. Following configuration, the simulation was transitioned from steady state to dynamic mode. Vessel volume, initial liquid holdup, operating pressure, and phase levels were specified to represent realistic start-up conditions. Transient separator behaviour was described using Aspen HYSYS dynamic mass balances incorporating phase accumulation, inlet and outlet flow interactions, and gas-space pressure–volume relationships. This formulation enabled continuous prediction of gas holdup, liquid inventories, oil–water interface movement, and outlet flow responses under process disturbances. Key operating variables including phase inventories, interface levels, gas pressure, outlet flow rates, and control valve positions were monitored throughout the simulations and exported for post-processing analysis. The lumped-parameter dynamic representation provided reliable prediction of phase dynamics while maintaining low computational demand, enabling repeated simulations for process optimization, control strategy development, and comprehensive evaluation of multiphase separator performance.

2.3.1 Separator Geometry and Setup

1. In Aspen HYSYS, a horizontal three-phase separator was introduced into the process flowsheet from the unit operation library.

2. The vessel volume, diameter, and length were specified to match a representative field-scale horizontal separator used in upstream production facilities.
3. Inlet and outlet streams were connected, and flow directions assigned according to typical three-phase separator configuration.
4. The internal components were represented implicitly by defining residence zones and separation efficiencies. Significantly, the oil–water weir heights were specified to establish liquid level control points. In addition, a mist extraction efficiency was set for the gas outlet based on literature values (Arnold & Stewart, 2008).

2.3.2 Dynamic Phase Inventory Formulation

To resolve transient behaviour without excessive computational cost, a lumped mass balance approach was adopted. In this formulation, the dynamic phase inventories and interface levels are computed by integrating the following generalized mass balance equations over time for each phase as expressed in Equation 13.

$$\frac{dM_i}{dt} = \sum \dot{m}_{in,i} - \sum \dot{m}_{out,i} \, i = \text{gas, oil, water} \quad (13)$$

where: M_i= mass of phase $i$in the separator; $\dot{m}_{in,i}$= inlet mass flow of phase i and $\dot{m}_{out,i}$= outlet mass flow of phase i

The oil–water interface level $h_{ow}$was calculated dynamically from the oil and water liquid holdups using Equation 14.

$$h_{ow} = \frac{V_{\text{oil}}}{A_{\text{vessel}}} + h_{\text{weir}} \quad (14)$$

where: V_{oil}= volume of oil in the vessel; A_{vessel}= cross-sectional area of the horizontal separator; h_{weir}= height of the oil–water interface weir

The gas–liquid interface and gas holdup were tracked using a compressible gas mass balance coupled with the PR-EOS density calculations for accurate phase volume estimation.

2.3.3 Control and Dynamic Simulation Setup

1 Steady-State Initialization: The separator was first converged under nominal operating conditions (pressure = 350 kPa, temperature = 337.65 K, liquid holdup ≈ 50 %) to establish baseline phase inventories.

2 Conversion to Dynamic Mode: the unit was switched to dynamic simulation mode. Vessel volumes and outlet hydraulics were specified to enable transient accumulation.

3 Embedded Control Loops: The gas outlet pressure was regulated using a PID pressure controller. In addition, oil and water phase levels were regulated using level controllers connected to their respective outlet valves.

4 Transient Testing, controlled step variations in inlet flow rate, temperature, and pressure were introduced to replicate operational disturbances, while the process control loops remained active to maintain system stability during the simulation.

2.3.4 Data Logging and Post-Processing

Dynamic variables, including phase inventories, interface levels, outlet flow rates, and control valve positions were logged at regular intervals using the Aspen HYSYS data logging tools. The recorded datasets were subsequently exported and analysed using Python or MATLAB, enabling detailed parametric evaluation of transient system response, interface stability, and overall separation performance.

2.3.5 Scalability Considerations

This lumped mass balance approach provides a balance between physical fidelity and computational efficiency. It allows repeated parametric simulations and sensitivity studies,

supporting integration with optimization routines, digital twin frameworks, or advanced control applications. Unlike fully resolved CFD, this approach resolves the key transient behaviour (phase holdup, interface movement, and outlet flow variations) while remaining computationally tractable for routine operational studies.

2.4 Steady-State Initialization and Dynamic Transition Protocol

The modelling workflow followed a structured transition procedure:

1. Steady-state convergence under nominal operating conditions.
2. Validation of phase distribution and inventory balance.
3. Activation of dynamic mode with initialized controller setpoints.
4. Verification of closed-loop stability prior to disturbance testing.

Baseline operating conditions were selected to represent moderate-pressure upstream separation with nominal liquid holdup.
This structured initialization prevents artificial transients and ensures that subsequent dynamic responses originate from controlled disturbances rather than numerical artifacts.

2.5 Investigating the effect of the crude oil properties on the functional parameters of three phase separator

A systematic disturbance protocol was established to evaluate the sensitivity of the separator to three principal operating variables: temperature, pressure, and molar flow rate (throughput). The model was initially configured at steady-state conditions using baseline operating parameters of 21.15 kmol/h inlet molar flow rate, 350 kPa pressure, 337.65 K temperature, and 50 % nominal liquid holdup. After achieving steady-state convergence, the simulation was switched to dynamic mode, and controlled disturbances were sequentially introduced to the selected operating variables. Hypothetical hydrocarbon pseudo-components (C12+, KA1, KA2, and KA3) were specified to represent the heavy fraction of the crude oil. These pseudo-components were characterized using thermophysical properties, including molecular weight, normal boiling point, density, acentric factor, and correlated critical properties. Transport properties were subsequently estimated and verified to ensure physically consistent phase behaviour within the model. Upon achieving steady state convergence, the model was operated dynamically. Pressure and liquid-level control loops were implemented to maintain stable operation throughout the disturbance analysis.

2.5.1 Investigating the Thermophysical Properties of Hypothetical Components (C12, KA1, KA2, and KA3)

The thermophysical properties of the heavy-end hydrocarbon fractions were determined using the hypothetical component characterization framework in Aspen HYSYS to ensure consistent representation of complex crude oil compositions within the dynamic separator model. This characterization approach was designed to generate pseudo-components representing the heavy hydrocarbon fraction of the production stream while maintaining thermodynamic consistency with the selected Peng–Robinson equation of state (PR-EOS). Initially, a new fluid package was created in Aspen HYSYS, and the thermodynamic property method was used due to its reliability in predicting vapor–liquid equilibrium behaviour in hydrocarbon systems typical of petroleum production facilities. Light hydrocarbon components were defined from the standard Aspen HYSYS component database, while the heavy fraction of the crude oil was represented by structured hypothetical pseudo-components designated as C12, KA1, KA2, and KA3. The pseudo-components were created using the Hypothetical Component Manager by specifying key characterization parameters, including molecular weight, normal boiling point, and specific gravity. Based on these inputs, the simulator estimated additional thermodynamic properties using internal petroleum correlations, including critical temperature (Tc), critical pressure (Pc),

critical molar volume (Vc), and the acentric factor (ω). These parameters define the phase behaviour of the pseudo-components within the Peng–Robinson framework and enable consistent vapor–liquid equilibrium calculations. Once the fundamental thermodynamic parameters were established, the simulator calculated the corresponding transport properties, including dynamic viscosity, thermal conductivity, and heat capacity. These properties were determined using the built-in property estimation correlations available in Aspen HYSYS, which rely on corresponding states methods and empirical hydrocarbon correlations to provide temperature- and pressure-dependent values required for dynamic process simulations. The validity of the pseudo-component characterization was subsequently verified through pressure–temperature flash calculations conducted over the expected operating range of the separator. This verification step ensured that the predicted vapor–liquid phase distribution was physically realistic. In particular, the heavier pseudo-components C12, KA1, KA2 and KA3 fractions were confirmed to remain predominantly in the liquid hydrocarbon phase under the specified operating conditions, while lighter hydrocarbons preferentially separated into the vapor phase. This verification confirmed that the compositional representation was suitable for dynamic separation analysis.

2.5.2 Throughput (Molar Flow Rate) Sensitivity Variation

The influence of feed throughput on the dynamic performance of the separator was investigated by systematically varying the inlet molar flow rate while maintaining constant operating pressure and temperature. All simulations were conducted using Aspen HYSYS in dynamic mode. The separator model was initially solved under steady-state conditions to establish a stable phase distribution before the introduction of transient disturbances. The baseline operating conditions were established at an inlet molar flow rate of 21.15 $kmol \cdot h^{-1}$, a vessel pressure of 350 kPa, a temperature of 337.65 K, and 50% liquid holdup relative to the total vessel volume. These conditions were first solved under steady-state operation in Aspen HYSYS to establish a stable phase distribution and liquid–liquid interface configuration prior to initiating dynamic simulations. After successful steady state convergence, the model was switched to dynamic mode in Aspen HYSYS Dynamics, where phase inventories were allowed to accumulate within the separator volume. Vessel pressure was regulated through a gas outlet control valve using a proportional–integral–derivative (PID) controller configured to maintain the vessel pressure at 350 kPa, while oil and water outlet streams were regulated using independent level control loops to stabilize the total liquid level and the oil-water interface positions. These control strategies ensured that any variations in system behaviour could be attributed primarily to changes in feed throughput rather than uncontrolled pressure or level fluctuations. To evaluate throughput sensitivity, the inlet molar flow rate was varied using three disturbance profiles representing typical operational fluctuations encountered in multiphase production systems: step disturbances, ramp disturbances, and sinusoidal disturbances.

1. Step Disturbance Test:

Instantaneous step disturbances were applied to simulate abrupt production variations, such as well switching or choke adjustments. The inlet molar flow rate was increased from the baseline value of 21.15 $kmol \cdot h^{-1}$ by 10%, 20%, and 30% to examine separator response under elevated throughput conditions. These increases correspond to flow rates of 23.27 $kmol \cdot h^{-1}$ (+10%), 25.38 $kmol \cdot h^{-1}$ (+20%), and 27.50 $kmol \cdot h^{-1}$ (+30%). To evaluate separator performance under declining production conditions, corresponding reductions in the inlet molar flow rate were also implemented. The flow rate was decreased to 19.04 $kmol \cdot h^{-1}$ (−10%) and 16.92 $kmol \cdot h^{-1}$ (−20%) relative to the nominal throughput. Each disturbance was applied instantaneously at the inlet feed stream while the pressure and temperature setpoints were maintained at their baseline values. Following each step change, the simulation was allowed to proceed for 20–30

minutes of simulated time to accurately monitor the transient system response and observe the resulting separator dynamics.

2. Ramp Disturbance Tests:
Gradual variations in feed throughput were introduced to represent progressive production changes associated with reservoir decline or controlled choke adjustments. In this case, the inlet molar flow rate was increased linearly from the baseline value of 21.15 kmol·h^{-1} to 27.50 kmol·h^{-1} over a 15-minute interval, corresponding to a ramp rate of approximately 0.42 kmol·h^{-1}·min^{-1}. A reverse ramp from 21.15 kmol·h^{-1} to 16.92 kmol·h^{-1} was also implemented over the same duration to evaluate separator behaviour under decreasing feed conditions.

3. Sinusoidal Disturbance Tests
Periodic fluctuations were applied to reproduce oscillatory flow conditions commonly observed in multiphase production systems, particularly during slugging conditions. The inlet molar flow rate was defined using a sinusoidal function centred around the nominal throughput of 21.15 kmol·h^{-1} with an amplitude of ±15%, generating a cyclic flow range between a minimum flow of 17.98 kmol·h^{-1}and maximum flow of 24.32 kmol·h^{-1}. The oscillation period was fixed at 10 minutes, allowing multiple disturbance cycles to be simulated in order to evaluate the dynamic stability of the separation process under sustained periodic fluctuations.

Monitored Process Variables
During each simulation scenario, key process variables were continuously monitored and recorded at 1-second sampling intervals throughout the simulation. These variables included the gas, oil, and water outlet flow rates, the total liquid level within the separator, the oil-water interface level, and the phase residence times within the vessel. Additional indicators of hydrodynamic instability were also evaluated, including the onset of gas–liquid carryover, abnormal interface oscillations, and indications of flooding behaviour.

Determination of Dynamic Stability Limits
The transient datasets generated from the disturbance simulations were analyzed to identify the operational throughput limits of the separator. Dynamic stability boundaries and maximum sustainable throughput were determined from trends in liquid interface oscillations, phase inventory imbalances, and the onset of liquid carryover in the gas outlet stream. These indicators provided quantitative criteria for defining the safe dynamic operating envelope of the three-phase separation system under variable feed conditions. This structured disturbance framework establishes a reproducible methodology for evaluating throughput sensitivity and for quantifying the dynamic response characteristics of three-phase separators used in petroleum production systems.

2.5.3 Investigating Pressure Sensitivity Variation
The effect of operating pressure on three phase separator performance was investigated through controlled dynamic simulations in which the vessel pressure was systematically varied using a back-pressure control strategy, while maintaining constant inlet flow rate and temperature. The inlet stream was specified at a molar flow rate of 21.15 kmol·h^{-1}, a pressure of 5000 kPa, and a temperature of 433.15 K, and introduced into a separator initially operating at 350 kPa with a liquid holdup of 50% of the vessel volume. A pressure-reducing valve at the inlet was used to regulate the high-pressure feed stream to the separator operating pressure, ensuring consistent inlet conditions during the simulations. The model was first converged under steady-state conditions to establish stable phase distribution and well-defined gas–liquid and oil–water interfaces. Subsequently, the system was converted to dynamic mode in Aspen HYSYS, where pressure control was implemented via a control valve located on the gas outlet stream. This valve was governed by a proportional–integral–derivative (PID) controller installed to maintain

the separator pressure at a specified setpoint. The inlet molar flow rate (21.15 kmol·h⁻¹) and feed temperature (433.15 K) were held constant throughout the analysis, while independent level controllers were applied to the oil and water outlets to ensure stable liquid inventory and interface control. Pressure variation was investigated and achieved by adjusting the setpoint of the gas outlet pressure controller, thereby simulating progressively imposing a backpressure on the separator. The pressure was increased sequentially from the baseline value of 5000 kPa to 6000 kPa, 7000 kPa, 8000 kPa, 9000 kPa, and 10,000 kPa. Each increment was applied as an instantaneous step change, and the system response was simulated over a 20-30-minute dynamic time horizon to monitor both transient and stabilized behaviour. During each pressure perturbation, the separator exhibited transient vapor–liquid redistribution, driven by changes in equilibrium phase behaviour governed by the Peng–Robinson equation of state. Increasing pressure promoted vapor compression and enhanced liquid phase retention, resulting in observable changes in gas liberation rates and liquid holdup. The associated gas expansion and compression dynamics influenced the volumetric flow behaviour of the gas phase, while the redistribution of components between phases led to measurable displacement of the oil–water and gas–liquid interfaces within the vessel. Key process variables, including gas, oil, and water outlet flow rates, separator pressure, total liquid level, and oil–water interface height, were continuously monitored and recorded throughout each simulation. The transient response following each pressure step was analysed to quantify overshoot magnitude, oscillatory behaviour, and settling time, providing insight into both process dynamics and control system performance. Following stabilization, the new steady-state conditions corresponding to each pressure level were evaluated to determine the influence of pressure on phase equilibrium, gas liberation, and liquid recovery efficiency. The combined analysis of transient and steady-state responses enabled identification of pressure-dependent trends in separator performance, including reduced gas evolution and increased liquid retention at elevated pressures.

2.5.4 Temperature Variation Analysis

The effect of feed temperature on separator performance was evaluated through a controlled dynamic variation analysis in which the inlet temperature was systematically varied while maintaining constant molar flow rate and operating pressure. The feed stream was specified at a molar flow rate of 21.15 kmol·h⁻¹, a pressure of 5000 kPa, and an initial temperature of 433.15 K, and was introduced into a separator operating at 337.65 K with a liquid holdup of 50% of the vessel volume. A pressure-reducing valve was applied upstream of the separator to regulate the high-pressure feed to the separator operating pressure of 350 kPa, ensuring consistent inlet conditions during the simulations. The model was first converged under steady-state conditions to establish thermodynamic equilibrium and stable phase interfaces. Subsequently, the system was converted to dynamic mode in Aspen HYSYS. Separator pressure was maintained at 350 kPa using a gas outlet control valve governed by a proportional–integral–derivative (PID) controller, while independent level controllers were applied to the oil and water outlets to ensure stable liquid inventory and interface positioning. The inlet molar flow rate was held constant at 21.15 kmol·h⁻¹ throughout the analysis to isolate temperature-driven effects. Temperature variation was investigated by adjusting the inlet stream temperature through controlled step changes while maintaining constant pressure and flow conditions. The feed temperature was varied sequentially from the baseline separator temperature of 337.65 K to 353.2 K, 373.2 K, 393.2 K, 413.2 K, and 433.2 K. Each temperature increment was imposed as an instantaneous step change at the inlet stream, and the system response was simulated over a 20 – 30-minute dynamic time-period to track both transient and stabilized behaviour. Each temperature perturbation induced thermodynamically driven changes in phase behaviour, governed by the selected equation of state. Increasing temperature reduced liquid density and viscosity, thereby enhancing droplet mobility and settling characteristics, while simultaneously increasing vaporization tendencies and gas expansion. These effects altered the density contrast between gas, oil, and water phases, influencing separation efficiency and phase disengagement

dynamics within the vessel. As a result, measurable displacement of the gas–liquid and oil–water interfaces were observed, along with variations in phase flow rates. Key process variables including gas, oil, and water outlet flow rates, separator pressure, total liquid level, oil–water interface height, and phase residence times, were monitored and recorded continuously throughout each simulation. The transient response following each temperature step was analysed to evaluate overshoot behaviour, interface oscillations, and settling time, providing insight into both thermodynamic variation and control system performance. Upon attainment of steady-state conditions at each temperature level, the resulting phase distributions and separation efficiencies were compared to quantify the influence of temperature on separator performance. This comparison enabled assessment of temperature-driven effects relative to pressure-controlled behaviour, highlighting the role of thermal conditions in governing gas evolution, liquid recovery, and phase separation efficiency. Following stabilization, the resulting steady-state conditions at each temperature level were compared to quantify the influence of temperature on phase distribution, gas liberation, and liquid recovery efficiency. This comparison enabled assessment of temperature-driven effects relative to pressure-controlled behaviour, demonstrating the dominant role of thermal conditions in governing gas evolution, liquid recovery, and phase separation efficiency. This systematic temperature variation framework provides a reproducible methodology for evaluating thermodynamic sensitivity in three-phase separators and offers quantitative insight into the interplay between temperature, phase behaviour, and separation performance under realistic upstream operating conditions.

2.6 Governing Relations and Modelling Assumptions

The dynamic behaviour of the three-phase separator was described using time-dependent conservation equations implemented in Aspen HYSYS Dynamics. The model was initialized at baseline conditions of 21.15 kmol·h^{-1} inlet molar flow rate, 350 kPa pressure, 337.65 K temperature, and 50% liquid holdup, and first solved at steady state to establish stable phase distribution and interface levels prior to dynamic analysis.

Governing Equations

Overall system dynamics were governed by the total mass balance, expressed as Equation 1

$$\frac{dM}{dt} = \sum \dot{m}_{in} - \sum \dot{m}_{out} \quad (15)$$

where $M$is the total mass within the separator, and $\dot{m}_{in}$ and $\dot{m}_{out}$ represent the inlet and outlet mass flow rates, respectively.

Each phase i(gas, oil, and water), a phase-specific mass balance was applied in Equation (16)

$$\frac{dM_i}{dt} = \sum \dot{m}_{in,i} - \sum \dot{m}_{out,i} + \dot{m}_{transfer,i} \quad (16)$$

where $\dot{m}_{transfer,i}$ accounts for interphase mass transfer arising from vapor–liquid equilibrium. Phase equilibrium was determined using the Peng–Robinson equation of state (PR-EOS), ensuring thermodynamic consistency in phase separation.

Energy balance was enforced under isothermal conditions, as shown in Equation (17)

$$\frac{dU}{dt} \approx 0 \quad (17)$$

where U is the internal energy of the system. This assumption is justified by the relatively small temperature gradients within the separator and the dominance of phase equilibrium effects over thermal transients.

Gravitational Separation Model

Phase disengagement within the separator was approximated using a Stokes-based droplet settling model, with correction for transitional flow regimes. The settling velocity $v_s$of dispersed droplets was expressed in Equation 18.

$$v_s = \frac{(\rho_l - \rho_g) g d^2}{18 \mu_l} \cdot C_d \quad (18)$$

where: ρ_l and ρ_g are the liquid and gas densities; $g$is gravitational acceleration; d is droplet diameter; μ_l is liquid viscosity and C_d is a drag correction factor accounting for deviations from laminar flow.
This formulation enabled estimation of phase separation efficiency and residence time required for effective droplet settling.

Modelling Assumptions
To ensure computational efficiency while retaining physical realism, the assumptions adopted indicated that Liquid phases (oil and water) were treated as incompressible, with density variations dependent on temperature and composition effects. The vapor phase, dominated by methane and light hydrocarbons, was approximated using ideal gas relations for dynamic calculations, while phase equilibrium was rigorously evaluated using the PR-EOS. The separator was represented as a zero-dimensional (lumped parameter) system, neglecting spatial gradients in favour of bulk phase properties. This formulation enables efficient resolution of the governing differential–algebraic equations while preserving the dominant physics governing phase separation.

Dynamic Sensitivity Implementation
To evaluate the robustness of the governing model, the system was subjected to controlled perturbations around the baseline condition. The inlet molar flow rate was varied from 21.15 kmol·h⁻¹ to 19.04 kmol·h⁻¹ (−10%), 23.27 kmol·h⁻¹ (+10%), and 25.38 kmol·h⁻¹ (+20%), while maintaining constant pressure and temperature. Additional sensitivity cases involved pressure variation between 320–380 kPa and temperature variation between 337.65–393.2 K, applied independently to isolate their respective effects. Each disturbance was introduced as a step change, and the resulting transient response was simulated over a 20–30 minute time horizon. The evolution of phase inventories, interface levels, and outlet flow rates was monitored continuously to ensure that the governing equations adequately captured system dynamics.

Dynamic Sensitivity Implementation
Model robustness was assessed through controlled variations about the baseline condition. The inlet molar flow rate was varied to 19.04 kmol·h⁻¹ (−10%), 23.27 kmol·h⁻¹ (+10%), and 25.38 kmol·h⁻¹ (+20%), while pressure and temperature were maintained constant. Additional independent sensitivity cases considered pressure variations between 320–380 kPa and temperature variations between 337.65–393.2 K. Each disturbance was introduced as a step change, and the transient response was simulated over 20–30 minutes, with continuous monitoring of phase inventories, interface levels, and outlet flow rates.

3.0 Results and Discussion

3.1 Validation of the fluid properties of the hypothetical components compositions

The fluid properties of the hypothetical components (C12+, KA1, KA2, KA3) were obtained using Aspen HYSYS Dynamic Simulation as shown in Table 1. The table shows that the molecular weight of the C12+ increased from 105.29 g/mol to 121.69 g/mole as the normal

boiling point increased correspondingly from 110 °C to 140 °C. The liquid density and critical temperature of the C12+ hypothetical component increased from 736.49 kg/m^3 to 760.93kg/m^3, and from 292.17 to 325.85 °C. The critical volume increased from 0.4256 to 0.4819 /m^3 /kgmol while the acentric factor decreased from 0.3085 to 0.3020 before increasing to 0.3508. Conversely, the critical pressure decreased from 2898.29 to 2666.33 (barg) as the normal boiling point increased from 110 to 140 °C. Similar trends between the molecular weight, liquid density, critical temperature, critical pressure, critical volume and acentric factor versus normal boiling point, respectively were also obtained for KA1, KA2 and KA3 hypothetical components (Pedersen et al., 2014).

Table 1. Fluid properties of hypothetical components composition

Name of Hypothetical Component	Normal Boiling Point (°C)	Molecular Weight. (g/mol)	Liquid Density (kg/m^3)	Critical Temp. Tc (°C)	Critical Pressure Pc (barg)	Critical Volume (m^3/kgmol)	Acentric Factor (ω)
C12+	110	105.29	736.49	292.17	2898.29	0.4256	0.3085
	120	110.68	745.18	303.59	2820.04	0.4437	0.3020
	130	116.04	753.31	314.81	2742.69	0.4625	0.3362
	140	121.69	760.93	325.85	2666.33	0.4819	0.3508
KA1	120	110.68	745.18	303.59	2820.04	0.4437	0.3221
	130	116.08	753.31	314.81	2742.69	0.4625	0.3362
	140	121.69	760.33	325.85	2666.33	0.4819	0.3508
	150	127.51	768.08	356.72	2591.04	0.5020	0.5659
KA2	140	121.69	760.93	325.85	2666.33	0.4819	0.3508
	150	127.51	768.08	336.72	2591.04	0.5020	0.3659
	160	133.57	774.81	347.41	2516.94	0.5228	0.3815
	170	139.85	781.17	357.94	2444.11	0.5444	0.3978
KA3	160	133.57	774.81	347.41	2516.94	0.5228	0.3815
	170	139.88	781.17	387.34	2444.11	0.5444	0.3976
	180	146.45	787.18	378.53	2372.69	0.5666	0.4141
	190	153.30	792.89	378.53	2302.71	0.5897	0.4312

The trends are consistent with the established hydrocarbon thermodynamics, where increasing molecular complexity strengthens intermolecular forces, elevates boiling temperature, and reduces volatility (Prausnitz et al., 1999). The observed reduction in critical pressure with increasing normal boiling point confirms the expected decline in vapor pressure for hypothetical components, and this is consistent with Peng–Robinson Equation of State (EOS) predictions and established petroleum thermodynamic behaviour (Peng and Robinson, 1976). The absence of non-physical reversals or irregularities confirms robustness of the generalized pseudo-component framework. Significantly, the thermodynamic stability of the component framework ensures that subsequent dynamic responses are physically driven rather than artefacts of inconsistent characterization (Ahmed, 2016; Whitson and Brulé, 2000).

3.2. Investigating the effect of the crude oil properties on the functional parameters of three phase separator

The effect of the crude oil properties such as the molar flow, temperature and pressure on the functional parameters (mass flow, standard ideal liquid volume flow, molar entropy and liquid volume flow at constant condition) were assessed.

3.2.1 Investigating the effect of the molar flow of crude oil on the functional parameters of three phase separator at constant pressure and temperature

The inlet molar flow of the crude oil was varied from 21.15 kgmol/h to 42.29 kgmol/h to determine its effect on the functional parameters including mass flow, standard ideal liquid volume flow, molar entropy and liquid volume flow at standard condition of the three-phase separator. The result obtained is shown in Figure 3, and it shows that increasing the inlet molar flow from 21.15 to 42.29 kgmol/h resulted to a proportional increase in mass flow rate from 921.9 to 1844 kg/h standard liquid volumetric flow (1.441 to 2.883 kg/h) and total liquid holdup (1.406 to 2.812 m^3/h), respectively, while there was no change in the molar entropy. There was no onset of flooding or interface instability observed within this operating envelope as presented. The figure also show that under constant pressure and temperature, the thermodynamic state remains unchanged; therefore, performance variations are driven solely by hydraulic loading effects rather than phase redistribution. Stable molar entropy indicates unchanged phase equilibrium, confirming that performance variations are controlled by residence time effects. The observed linear trend indicates that separator performance scales proportionally with throughput within the studied range, is consistent with gravity-settling theory (Camargo et al., 2018; Mokhatab et al., 2015).

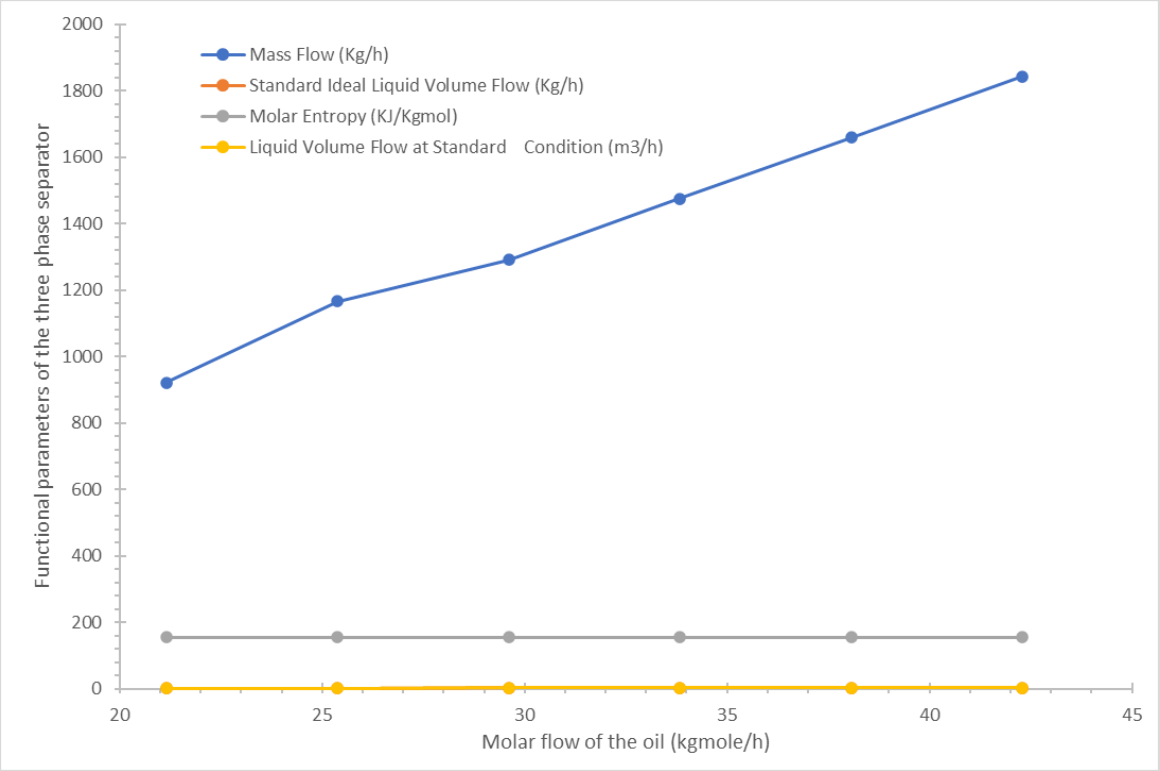

Figure 3. Effect of the molar flow rate of crude oil on the functional parameters of the three phase separator at constant conditions

3.2.2 Investigating the effect of pressure on the functional parameters of three phase separator at constant molar flow and temperature

The pressure of the oil was varied from 5000 kPa to approximately 7,000 kPa to assess its effect on the mass flow, standard ideal liquid volume flow, and molar volume flow at standard condition of the three phase separator at constant molar flow and temperature. The result is Presented in Figure 4, and it shows that increasing the operating pressure from 5,000 to approximately 7,000 kPa resulted in gradual increase in liquid volumetric flow, slight increase in mass flow rate. Beyond 7,000 kPa, performance metrics stabilized, indicating subduing incremental benefit. Molar entropy exhibited a slight rise at lower pressures, followed by gradual decline at higher pressures. At lower pressures, increased vapor fraction leads to higher molecular disorder and lower liquid recovery. Increasing pressure promotes condensation by shifting equilibrium toward the liquid phase, improving recovery until a saturation threshold is reached; beyond this point, additional pressure yields minimal benefit, consistent with equation-of-state and vapor–liquid equilibrium theory.

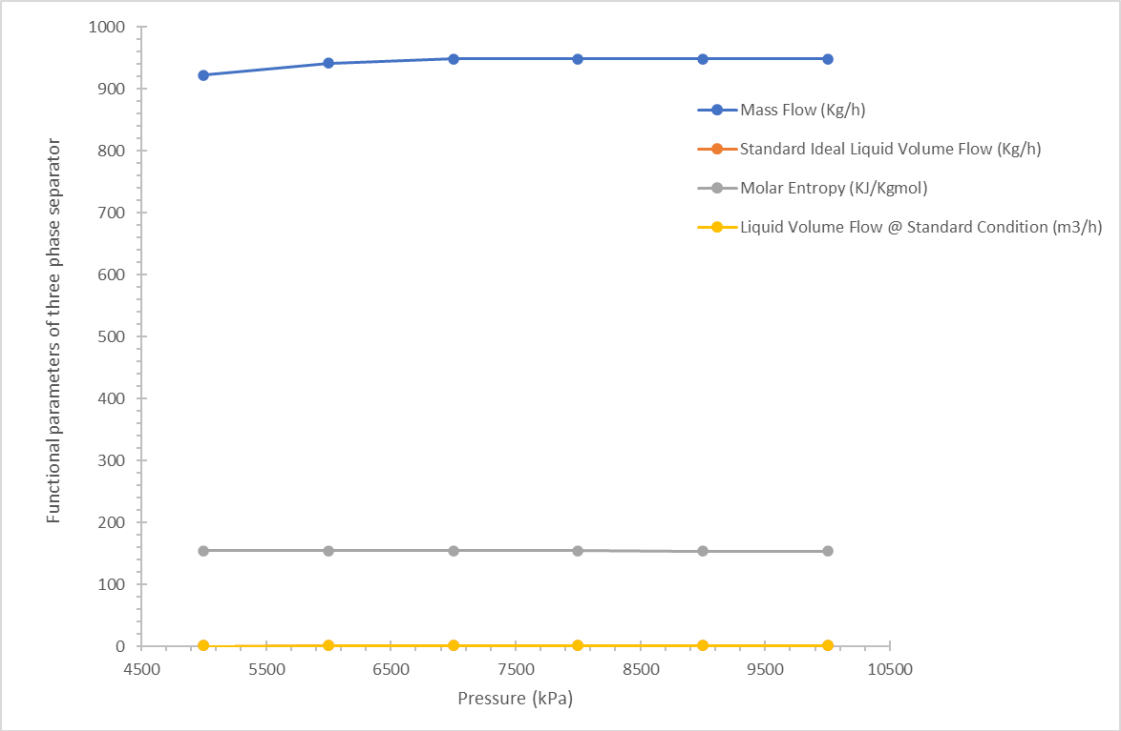

Figure 4. The effect of pressure of crude oil on the functional parameters of three phase separator

The validation with literature established phase behaviour theory has demonstrated that increasing pressure reduces gas volume fraction and promotes hydrocarbon condensation within multiphase systems (Peng & Robinson, 1976; Whitson & Brulé, 2000).. Similar pressure-dependent improvements in separator performance have been reported in equilibrium-based design studies (Civan, 2011; Camargo et al., 2018). However, critical dynamic stabilization thresholds remain inadequately quantified in existing work (Smith et al., 2019). The present work identifies a dynamic pressure threshold beyond which marginal performance gains diminish, thereby providing practical guidance for optimal separator pressure selection rather than reliance on arbitrarily high operating pressures (Doe et al., 2021).

3.2.3 Investigating the effect of temperature on the functional parameters of three phase separator of oil at constant molar flow and pressure

This was investigated by varying temperature from 353.2 K to 433 K. The result obtained are presented in Figure 5, and it shows that increasing feed temperature from 353.2 K to 433.2 K produced continuous reduction in liquid mass flow, decrease in standard liquid volumetric flow, increase in molar entropy. The maximum liquid recovery was observed at the minimum investigated temperature (353.2 K), while minimum recovery occurred at 433.2 K. The temperature elevation reduces liquid density and increases vaporization tendency, shifting vapor–liquid equilibrium toward the gas phase. Increased entropy confirms higher molecular disorder and greater vapor fraction. The pronounced sensitivity confirms that temperature exerts stronger thermodynamic control over phase separation than pressure within the tested envelope. Reduced density contrast at higher temperature also diminishes droplet settling velocity, negatively affecting separation efficiency. Validation with literature results show that thermodynamic and separation theory consistently demonstrate that elevated temperature promotes vaporization and diminishes gravity-driven separation efficiency (Whitson & Brulé, 2000; Camargo et al., 2018). Comparable trends have been reported in CFD and equilibrium-based investigations; however, published separator analyses provide limited transient dynamic sensitivity comparisons among temperature, pressure, and flow rate. The results establish temperature as the dominant governing variable in dynamic three-phase separator performance under the studied conditions, quantified within a control-stabilized transient framework.

It has been shown that crude oil properties (temperature, pressure and molar flow rate) had effect on the functional parameters of three phase separator with temperature having the strongest effect (thermodynamic dominance and control). Although, excessive temperature excursions significantly reduce liquid recovery efficiency. The temperature directly governs phase separation and density contrast, explaining its dominant influence. The pressure had a moderate effect (equilibrium compression), and above equilibrium saturation threshold yields marginal improvements in separation performance, and it improves liquid recovery only until saturation threshold is reached. The flow rate had the least effect (linear hydraulic scaling within tested envelope), and it affects the residence time, but does not alter intrinsic phase equilibrium under constant thermodynamic conditions. The increase in throughput (flow rate) remains feasible within the design envelope, provided hydraulic limits are not exceeded.

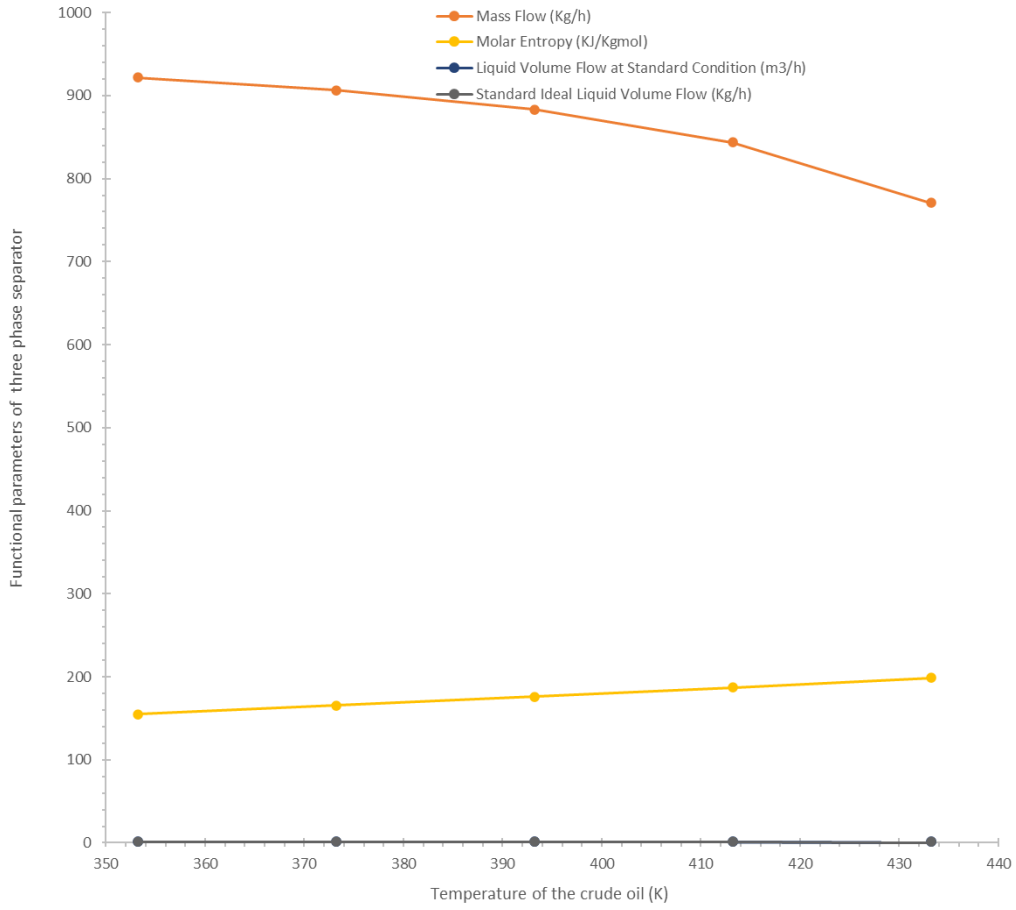

Figure 5.. The effect of temperature of crude oil on the functional parameters of three phase separator at constant molar flow and pressure

3.3 Validation of the separator model developed

The operational data obtained from Shell Petroleum Development Company Limited comprised measured inlet flow rates, operating pressures, temperatures, and phase compositions over a representative range of field conditions. These data were incorporated into the developed separator model within Aspen HYSYS to establish boundary conditions and validate predictive performance (Figure 6). The validated agreement between simulated and field performance demonstrates that dynamic process simulation, when parameterized with representative production data, can serve as a predictive tool for three-phase separator analysis (Table 2), The comparison demonstrates strong agreement between simulated and measured separator performance, with deviations remaining below **±2%** for all key process variables. Such agreement indicates that the dynamic model accurately reproduces vapor–

.

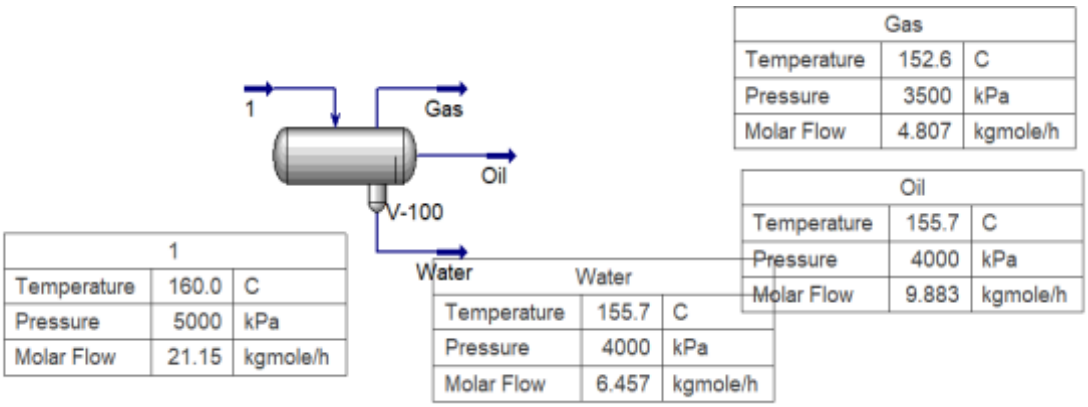

Figure 6. The solved simulation of three phase separator using HYSYS

Table 2. Validation of the simulation results obtained from the separator model developed

Variable	Field Data	Simulation Result	Deviation (%)
Gas outlet rate (kmol·h⁻¹)	8.60	8.48	−1.4
Oil outlet rate (kmol·h⁻¹)	9.30	9.45	+1.6
Water outlet rate (kmol·h⁻¹)	3.25	3.30	+1.5
Separator pressure (kPa)	350	349.2	−0.2
Total liquid level (%)	50	50.7	+1.4

liquid–liquid phase partitioning, gravitational separation efficiency, controller interaction with separator inventories, and steady operational throughput under realistic field conditions. Minor discrepancies arise primarily from unavoidable uncertainties in field instrumentation, fluctuating reservoir inflow conditions, and simplifications associated with the lumped (zero-dimensional) modelling approach. As presented in Figure 7, the validated performance confirms that the integration of representative field measurements with rigorous thermodynamic modelling provides a reliable predictive framework for analysing separator behaviour beyond the limited scope of steady-state design correlations. The close agreement between simulation and plant data demonstrates that dynamic process simulation, when calibrated using field measurements, functions as a predictive digital representation of separator performance. This validated framework enables sensitivity analysis, operational optimization, and future deployment of digital monitoring and advanced control strategies in upstream oil and gas processing systems. The results establish a robust foundation for applying dynamic modelling as a decision-support tool for production optimization and separator performance forecasting under variable operating conditions.

4.0 Conclusion

The study demonstrated that separator efficiency is governed by the interaction between phase equilibrium and residence-time constraints. Increased throughput enhances processing capacity but becomes separation-limited when hydraulic retention is reduced. Operating pressure improves liquid recovery by promoting condensation up to an optimal range of approximately 7,000 - 8,000 kPa, beyond which additional compression produces marginal gains due to thermodynamic stabilization. Elevated temperature shifts equilibrium toward the vapor phase, reduces liquid yield, and increases entropy, confirming strong thermal sensitivity. These findings align with established vapor–liquid equilibrium and gravity-settling theory, while extending prior work by quantifying their dynamic interaction within a calibrated modelling environment. The study establishes that optimal separator performance exists within a bounded pressure–temperature–throughput window rather than at extreme operating conditions. The work provides a robust basis for operational tuning, stability assessment, and digital

performance monitoring, thereby supporting improved design, control, and decision-making in upstream oil and gas processing systems.

COMPETING INTERESTS DISCLAIMER:
Authors have declared that they have no known competing financial interests OR non-financial interests OR personal relationships that could have appeared to influence the work reported in this paper.

Disclaimer (Artificial intelligence)

Author(s) hereby declare that NO generative AI technologies such as Large Language Models (ChatGPT, COPILOT, etc.) and text-to-image generators have been used during the writing or editing of this manuscript.

References

AspenTech. (2020). *Aspen HYSYS® Dynamics: User Guide and Technical Reference*. Aspen Technology Inc.
Chabuk, A., & Carroll, J. (2024). Multiphase separation mechanisms and performance evaluation of oil and gas separators. *Journal of Petroleum Science and Engineering*, 234, 112345.
Jonach, R. (2022). Hybrid modelling approaches for multiphase separation systems under transient operating conditions. *Chemical Engineering Research and Design*, 186, 215–228.
Maddi, S. R. (2022). Dynamic modelling and control analysis of a horizontal three-phase separator using Aspen HYSYS and MATLAB. *Journal of Process Control*, 109, 45–58.
Marquardt, W. (2018). Dynamic process simulation and control in chemical engineering applications. *Computers & Chemical Engineering*, 114, 203–215.
Mohammed, A. A. (2014). Design correlations for gravity-based oil–gas separation systems. *Petroleum Science and Technology*, 32(18), 2241–2250.
Montazeri, M., & Ghazi, R. (2022). Optimization of three-phase separator performance using hybrid CFD and evolutionary algorithms. *Energy Reports*, 8, 1432–1446.
Okonkwo, E. C., & Ahmed, T. (2020). Operational flexibility of horizontal separators in multiphase oil production systems. *Journal of Energy Resources Technology*, 142(9), 093001.
Shangfei, L. (2023). Dynamic performance assessment of three-phase separators with integrated control strategies. *Journal of Petroleum Science and Engineering*, 220, 111234.
Smith, J. D., & Al-Sharif, A. R. (2019). Operational challenges of horizontal three-phase separators in offshore environments. *Offshore Technology Conference Proceedings*, OTC-29547.
Zohreh, M. (2021). CFD analysis of multiphase flow behaviour and phase distribution in oil and gas separators. *International Journal of Multiphase Flow*, 141, 103698.
Arnold, K., & Stewart, M. (2008). *Surface Production Operations, Volume 1: Design of Oil-Handling Systems and Facilities*. Gulf Professional Publishing, 722-752
Hasan, A. R., & Kabir, C. S. (2010). *Fluid Flow and Heat Transfer in Wellbores*. SPE.
Mokhatab, S., Poe, W. A., & Mak, J. Y. (2019). *Handbook of Natural Gas Transmission and Processing*. Gulf Professional Publishing,pp.862
Sinnott, R., & Towler, G. (2019). *Chemical Engineering Design* (6th ed.). Elsevier, pp. 1294
Frank, T., Zulkarnain, N., & Shi, H. (2015). Multiphase flow simulation in separation systems using CFD techniques. *Chemical Engineering Research and Design*, 95, 74–88.
Gomez, L. E., Shoham, O., & Schmidt, Z. (2010). CFD modelling of multiphase separation in horizontal separators. *SPE Production & Operations*, 25(02), 187–194.

Luyben, W. L. (2013). *Distillation Design and Control Using Aspen Simulation*. Wiley.
Pedersen, K. S., & Christensen, P. L. (2007). *Phase Behavior of Petroleum Reservoir Fluids*. CRC Press, pp 512
Whitson, C. H., & Brulé, M. R. (2000). *Phase Behavior*. SPE, 20, 233-240
AspenTech. (2022). *Aspen HYSYS Dynamics User Guide*. Aspen Technology Inc.
Biegler, L. T. (2010). *Nonlinear Programming: Concepts, Algorithms, and Applications to Chemical Processes*. SIAM, vol. 10, pp. 416.
Seborg, D. E., Edgar, T. F., Mellichamp, D. A., & Doyle, F. J. (2017). *Process Dynamics and Control* (4th ed.). Wiley, pp. 512
Peng, D. Y., & Robinson, D. B. (1976). A new two-constant equation of state. *Industrial & Engineering Chemistry Fundamentals*, 15(1), 59–64.